Science of Sintering, **45** (2013) 341-350

doi: 10.2298/SOS1303341C

UDK 546.284;548.73

Creating of Highly Active Calcium-Silicate Phases for Application in Endodontics

B. Čolović, V. Jokanović, N. Jović

Institute for Nuclear Sciences "Vinča", University of Belgrade, Belgrade, Mike Petrovića Alasa 12-14, 11351 Belgrade, Serbia

Abstract:

The synthesis of active silicate phases by combined sol gel and high-temperature self-propagating wave method, is described in this paper. They show a significant decrease of setting time and good mechanical properties, which are very important for its potential application in endodontic practice.

Particularly, process of hydration of calcium silicate phases is carefully analyzed, from the aspect of phase changes during their soaking in water for 1, 3, 7 and 28 days. XRD and FTIR methods were used for phase analysis of all samples, while morphological characteristics and chemical composition of the given phases were investigated by SEM and EDS.

Key words: *Calcium Silicates, Endodontics, Setting Time, Compressive Strength, XRD.*

1. Introduction

Mineral trioxide aggregate (MTA) is a material with broad indications in endodontics. It is used in the treatment of various perforations of the root canal, pulpotomy and treatment of vital pulp as well as an apical barrier in teeth with necrotic pulp and open apex [1, 2].

Numerous investigations on direct pulp capping in permanent teeth were performed in order to evaluate formation, quality and thickness of calcified bridges, presence of inflammatory cells, and the efficiency of pulp protection as important criteria for assessing pulp vitality after the treatment. Comparative analysis of MTA and $Ca(OH)_2$ as materials for direct pulp capping, pointed to the significant differences. After application of MTA, the appearance of calcified bridge was observed after only one week [1, 2], while for $Ca(OH)_2$ this time was much longer (up to five months). Beside, the increasing number of inflamed pulps in the $Ca(OH)_2$ treated cases was caused by formation of voids between dentin bridges and medicament interface. This facilitated the entrance of irritants through dentin bridges toward the pulps over tunnel defects. Also, bacterial micro leakages at restoration margins induce the pulp inflammation [3-5].

Therefore, MTA is considered to be a potentially ideal material for perforation repair, retrograde filling, apexification and vital pulp therapy [6]. Several *in vitro* and *in vivo* studies have demonstrated that the sealing abilities of MTA are superior to those of amalgam, IRM and super EBA [1, 6-9]. However, some researchers had shown several very important disadvantages of MTA, related to its very long setting time and week rheological properties, due to which the results during its application may be non-consistent. Besides, particle size,

*) **Corresponding author**: dusanm@vinca.rs

powder to liquid ratio, temperature and presence of air in the mixture may influence the physical properties of MTA. During hydration in acidic environment, the weakening of the material structure was also noticed [9]. Therefore, any material with similar composition which shows higher degree of activity of silicate phases is welcome.

The synthesis method, described in this paper, based on the combination of sol-gel process and self-propagating synthesis, can significantly improve setting time of obtained calcium silicate phases (CS), through their accelerated hydration. Such kind of synthesis of silicate phases, to the best of our knowledge, is original and for the first time applied in literature. The process of material hydration, as the most responsible for its behavior, was carefully investigated.

2. Material and Methods

2.1. Synthesis and characterization methods of obtained inorganic phases

The calcium silicates were synthesized as follows: $CaCl_2 \cdot 5H_2O$ (Merck, Germany) and silica sol obtained by hydrothermal treatment were used in stoichiometric quantities (42.41 g of $CaCl_2 \cdot 5H_2O$ and 15 g of 30% silica sol solution [10], corresponding to the ratio Ca_3SiO_5: 2β-$CaSiO_4$ (C_3S: β-C_2S) = 2:1) to obtain silicate active phase. $Al(C_2H_3O_2)$ was added to the mixture to provide the production of small amount (3.01 %) of active C_3A phase. In order to start the combustion reaction [11], ammonium nitrate (NH_4NO_3), as an oxidation agent, and citric acid ($C_6H_8O_7CH_2O$), as a fuel, were added to the mixture.

First, the mixture of silica sol and $CaCl_2 \cdot 5H_2O$ was dried at 80 °C until the gel is obtained, and then was heated at 150 °C to remove water among the silica particles. As the water was evaporating, the silica gel was becoming more and more viscous, reaching high viscosity level at the end of reaction. In the next stage, the temperature was increased to 180 °C and the ignition the gel happened. The gel swelled into foam during the strong reaction of self-propagating combustion. The black ashes were obtained as a product of auto-ignition. During the combustion, a large volume of the gaseous products released and thus dissipated the heat and limited the temperature rise. This is important because it reduces the possibility of premature local partial sintering among the primary particles, which is important for maintaining the final powder activity. After this the sample was exposed to the thermal treatment at high temperatures and was quickly cooled using cooper plates, in order to obtain a high reactivity and low crystallinity of β-C_2S and C_3S phases. Finally, the resulting black powder, which contained some carbon residues, was calcined in air at 650°C for 4 h to obtain the desired products with small crystallite sizes. In order to obtain the final silicate phases, powder was additionally milled after the calcination.

CS were then mixed with water (water-to-powder ratio about 1:2) and compacted using a stainless steel plunger. Cement was allowed to set up to 28 days at 37 °C in sealed polyethylene containers.

Phase compositions of each sample were analyzed before soaking in water and 1, 3, 7 and 28 days after soaking using X-ray diffractometry, XRD (Philips PW 1050, Almelo, The Netherlands), with Ni–filtered Cu-K$\alpha_{1,2}$ radiation. The patterns were registered in the 2θ range 9-67° with a scanning step size of 0.02°. IR analysis (Nicollet 380 FT-IR, Termo Electron Corporation) was done for the sample before soaking and for samples soaked for 7 and 28 days. The morphology and the agglomerate size distribution of the milled powders were studied using scanning electron microscopy, SEM (JEOL, JSM-5300,Tokyo, Japan) under vacuum pressure of $1.33 \cdot 10^{-3}$ Pa and voltage of 20 kV. EDS (energy dispersive analysis) measurements were performed in order to detect chemical homogeneity of obtained phases and ratio of Ca and Si in various areas of silicate active phase.

3. Results and discussion

3.1. Phase and structural analysis of CS phases before soaking in water

XRD. X-ray diffraction patterns of C3S and β-C_2S phases of the given CS system are shown in Fig. 1.

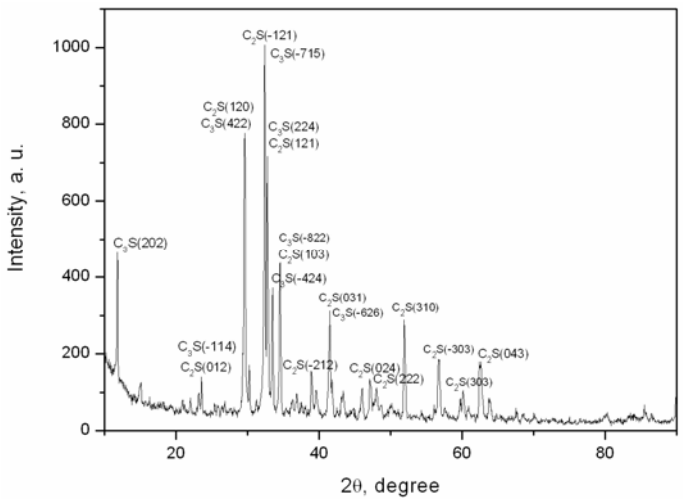

Fig. 1. XRD patterns of CS phases

The peaks at angles 11.7, 23.6, 29.6, 32.5, 32.8, 33.4, 34.6 and 41.5° (with corresponding planes: (-401), (-114), (422), (-715), (224), (-424), (1004) and (-626), respectively) correspond to C_3S phase, while peaks at angles 23.3, 29.7, 32.3, 33, 34.6, 41.6, 46.9, 51.9, 56.8, 60.2 and 62.7° (with corresponding planes: (012), (120), (-121), (121), (103), (031), (024), (310), (-303), (303) and (043), respectively) corresponded to β-C_2S phase. Based on Sherrer equation (calculated for highly pronounced planes at 32.1° (plane -121) for β-C_2S and (plane -715) for C_3S), the obtained values of crystallite sizes of these phases were about 19.9 nm.

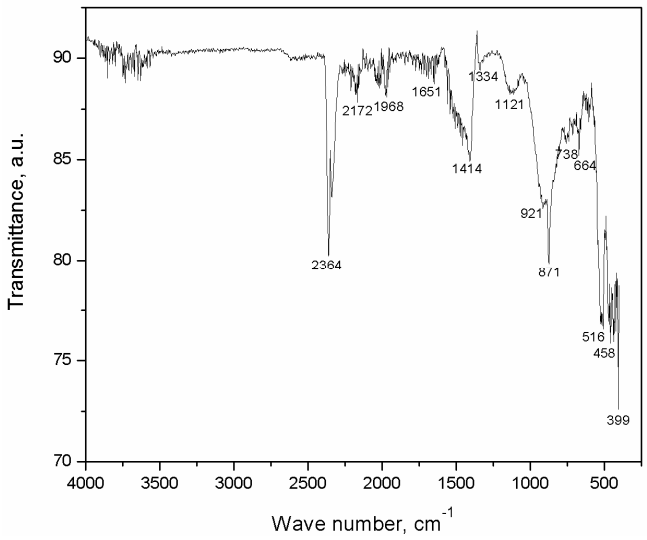

Fig. 2. FT-IR spectrum of CS phases

FTIR. The FTIR spectrum of CS phases is shown in Fig.2. The characteristic sharp and pronounced band at 2364 cm^{-1} and 2334 cm^{-1} can be probably assigned to the combination of band at 871 cm^{-1} and broad band at 1414 cm^{-1}. This characteristic doublet recorded between 2334 and 2364 cm^{-1} can be assigned to the stretching vibration of OH groups, and explained

by the corresponding decrease in hydrogen bond length, caused by steric effects [10, 12]. According to this explanation, fine structure of these bands may be generated by a strong anharmonic coupling mechanism, with the most prominent role of the high frequency proton stretching vibrations, anharmonically coupled with the low frequency hydrogen bond stretching vibration [12, 13]. The band at 2172 cm^{-1} can be assigned to SiH stretching mode in the small grains, gradually exposed to oxidation developed during combustion process at intermediate temperature during the synthesis of given phases. This is some kind of fingerprints of the oxidation state of silica during synthesis of these powders [10]. The band at 1968 cm^{-1} corresponds to SiO_2 vibrational modes [12].

The band at 1651 cm^{-1} can be ascribed to the liberation mode of OH, while the broad and unresolved asymmetric band with a minimum at 1414 cm^{-1} may be ascribed to vibrations corresponding to partially hydrated C_3S and C_2S phases. This band and band at 1334 cm^{-1} can be also assigned to the splitting of ν_3 vibration of calcium carbonate obtained on the surface of the silicate particles, influenced by adsorption of CO_2 from atmosphere during the synthesis (exposure of C_3S and C_2S mixture to CO_2 results very quickly in its surface carbonation) [14]. The bands at 1334 cm^{-1} region and 871 cm^{-1} observed in spectrum come from asymmetric stretch and out-of-plane bending of the C-O, respectively, and the medium intensity one at 738 cm^{-1} is due to angular bending of the O-C-O. The band at 1121 cm^{-1} can be assigned to vibration of C_2S units, while small band (shoulder) at 921 cm^{-1} can be indication of slight hydration of C_3S or C_2S [15, 16]. This factor is probably responsible for the appearance of a small band at 458 cm^{-1}. Generally, the spectra show that, as the C/S ratio increases, the broad band at around 940 cm^{-1} not only becomes narrower but also shifts to higher wave numbers, due to stretching vibration of the SiO_4. In addition, a weak band in the 1600-1500 cm^{-1} region appears, whereas the 500 cm^{-1} band almost disappears. The band at 940 cm^{-1} shifted to 960 or 989 cm^{-1} (whereas the band at 878 cm^{-1} remains unaffected) is an indication of hydration of C_3S [15, 16]. The shifting of the band at 940 cm^{-1} to higher wave number in the C-S-H suggests the possibility of continuous changes in the C_3S structure as the hydration takes places. The chemical environment of the bending vibrations of the bonds changes as hydration occurs. This factor is probably responsible for the appearance of a well-defined band at around 460 cm^{-1}. The band at 664 cm^{-1} can be attributed to the Si-O-Si symmetric vibration and band at 516 cm^{-1} to the out-of-plane bending vibration of SiO_4 [15, 16].

SEM and EDS. Structure of calcium silicate, as it is shown in Fig. 3, consists preferentially of agglomerates with sizes of the several micrometers, built up from smaller particles which dimensions are between 117 and 477 nm. These particles are preferentially of spherical or ellipsoidal shape, more or less elongated along one direction.

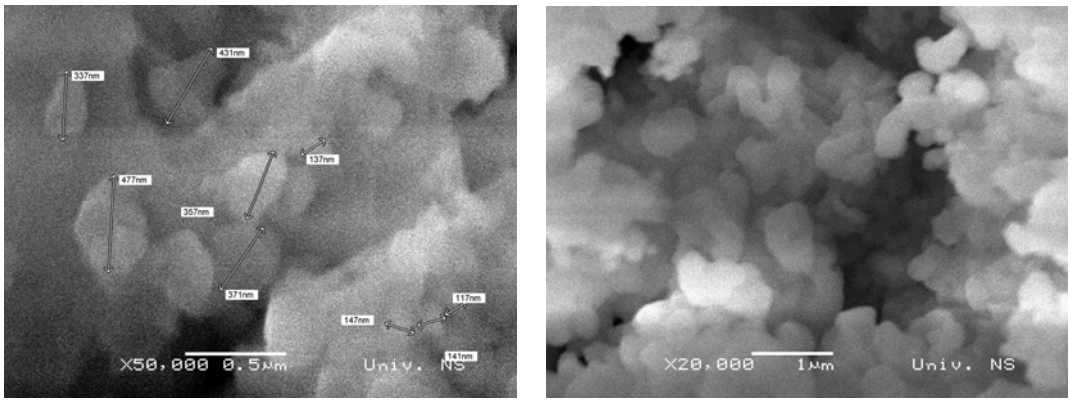

a) b)

Fig. 3. Typical appearance of calcium-silicate agglomerates and particles

EDS picture of typical spot (Fig. 4) shows that chemical composition of calcium

silicate (Ca- 22.21; Si- 8.22 and O- 69.7 at. %) corresponds to ratio Ca: Si of approximately 2.7:1 (at. %). Simple calculation can show that this value is close to the theoretical ratio of Ca: Si (2.66:1), for given mixture, corresponding to the ratio C_3S/C_2S=2:1), showing obviously homogenous distribution of both these phases within the sample. Comparing particle sizes obtained by SEM and crystallite sizes obtained from XRD spectra, it is clear that these particles consist of smaller building elements (crystallites), showing a significant potential activity of this system. Structures built on three hierarchical levels (agglomerates, particles and crystallites) may be promising because they cannot be biologically destructive (dimensions of agglomerates are not comparable with channels inside of cell membranes), whereas their nano-elements (nano crystallites) enable them very pronounced activity, important for quick bonding of these mixtures in endodontic therapy.

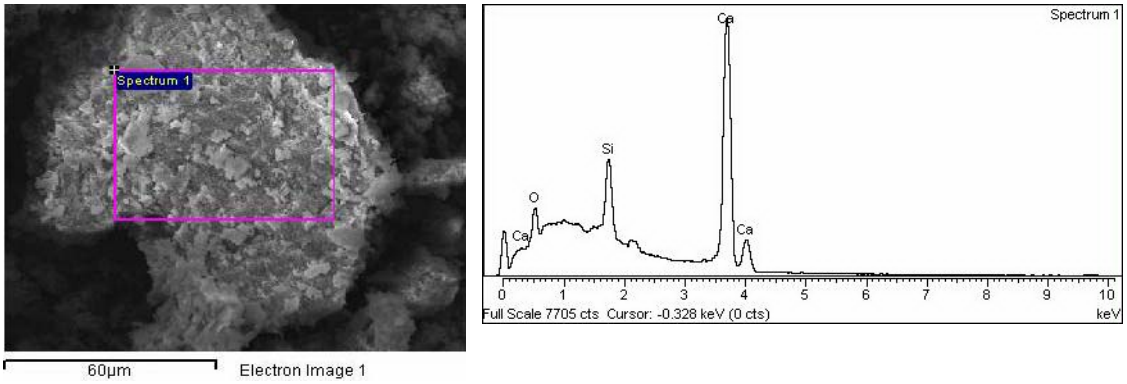

a) b)

Fig. 4. a) SEM micrograph of chosen spot of calcium silicate particles, with b) Typical EDS spectra

3.2. Hydration of calcium silicates

XRD. From XRD patterns for samples hydrated for 1, 3, 7 and 28 days (Fig.5), it is obvious that the quantity of hydrated phase tobermorite relative to sum of β-C_2S and C_3S phases was quite different, depending on the hydration time.

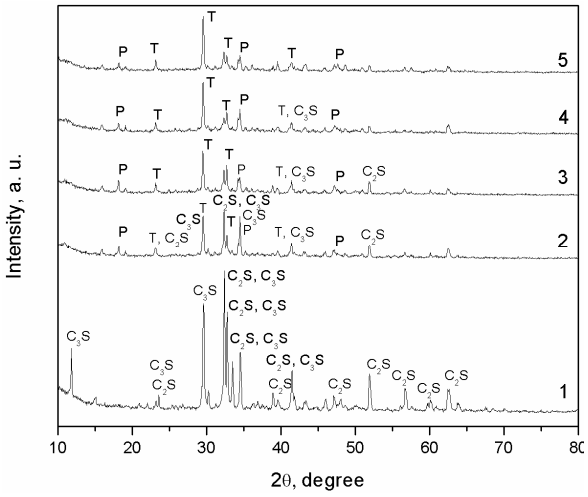

Fig. 5. XRD patterns of hydrated calcium silicates: 1- nonhydrated sample, 2- sample hydrated for 1 day, 3- sample hydrated for 3 days, 4- sample hydrated for 7 days, 5- sample hydrated for 28 days (T-tobermorite, P-portlandite)

For the sample hydrated for 1 day, beside the presence of hydrated phase of tobermorite (planes (006), (112), (202) and (213)) and portlandite (planes (011), (012) and (001) which showed the progress of hydration; significant amounts of β-C_2S and C_3S were noticed (the diffraction planes (012), (-121) and (310) for β-C_2S and (422), (-715), (1004) and (-626) for C_3S remained pronounced. For the sample hydrated for 3 days, only the plane (-626) corresponding to C_3S and the plane (310) corresponding to β-C_2S were present, but their diffraction intensity was decreased. This trend was continued and for the sample hydrated for 7 only the plane (-626) corresponding to C_3S was present, while the peaks of the main hydrated phase- tobermorite were more pronounced. Finally, for the sample hydrated for 28 days, β-C_2S and C_3S phases were completely transformed into the tobermorite, with small amounts of portlandite because the rest of $Ca(OH)_2$ was present as amorphous phase.

FTIR. FT-IR spectra of hydrated calcium silicates are shown on Fig.6. The bands at 3726 cm^{-1} (sample hydrated for 1 day (S-1)) and 3718 cm^{-1} (sample hydrated for 28 days (S-28)) indicates the presence of the 1.4 tobermorite which contains poorly resolved band in the range of 2800–3700 cm^{-1} due to larger content of molecular H_2O, compared to 1.1 nm tobermorite. This result is expected from its larger basal spacing. The bands at 3726 cm^{-1} and 3718 cm^{-1} can be assigned to vibrations which involve less hydrogen bonded protons in water molecules, including intensity corresponding to Ca-OH groups in the structure. The weak bands at 3740 cm^{-1} can be also assigned to Si–OH vibrations. The bands at 2997, 2938 and 2880 cm^{-1} (S-1), and 2990, 2938 and 2872 cm^{-1} (S-28), due to corresponding investigations of Cong and Kirkpatrick (1996), also proved the presence of tobermorite 1.4 nm.

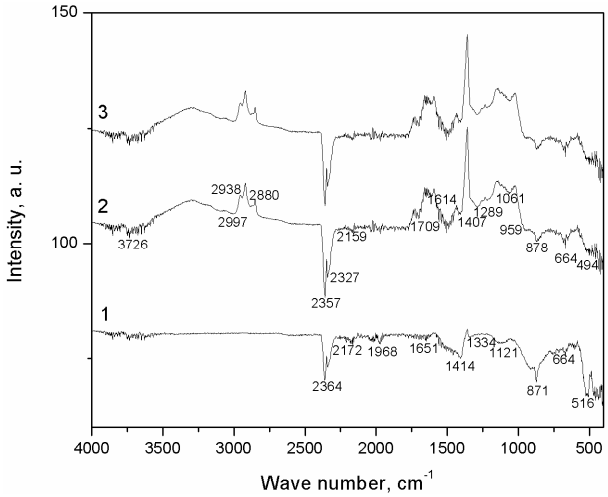

Fig. 6. FT-IR spectra of hydrated calcium silicates: 1- nonhydrated sample, 2- sample hydrated for 1 day, 3- sample hydrated for 28 days

The characteristic sharp and pronounced band at 2357 cm^{-1} can be assigned to combination of bands at 959 cm^{-1} and broad band 1407 cm^{-1}, the band at 2327 cm^{-1} to the combination of bands at 1407 cm^{-1} and 878 cm^{-1} while the band at 2364 cm^{-1} probably belongs to the combination of bands at 1489 cm^{-1} and 871 cm^{-1}. This characteristic doublet recorded between 2327 and 2357 cm^{-1} (S-1) and 2364 and 2320 cm^{-1} (S-28) can be stretching vibration of OH groups, and explained by the corresponding decrease in hydrogen bond length, caused by steric effects. The weak bands at 1407 and 1458 cm^{-1} and its combination, and overtone bands observed at 2997, 2938 and 2880 cm^{-1} (S-1) and 2990, 2938 and 2872 cm^{-1} (S-28) and week vibrations at 1407 and 1414 cm^{-1} indicate the presence of carbonate species in the samples. The band at 1614 cm^{-1} belongs to the water bending vibration. In the sample hydrated for 28 days two bending water vibrations are noticed. According to the above given explanation, fine structure of these bands may be generated by a strong anharmonic coupling

mechanism, with the most prominent role of the high frequency proton stretching vibrations, anharmonically coupled with the low frequency hydrogen bond stretching vibration. The bands at 2159 cm^{-1} (S-1) and 2165 cm^{-1} (S-28) can be assigned to SiH stretching mode in the small grains, gradually exposed to oxidation during combustion process at intermediate temperature during synthesis given phases. This is some kind of fingerprints of the oxidation state of silica during synthesis of these powders. The bands at 1709 cm^{-1} and 1702 cm^{-1} correspond probably to water bending vibration inside of gypsum dehydrate contained in small amount of samples. The band at 1216 cm^{-1} (S-28) can be assigned to the Si-O stretching vibrations in Q3 site, characteristic for presence of 1.1 nm tobermorite, while the bands at 1061 and 1054 cm^{-1} belong to the Si-O stretching vibrations in Q2 site of 1.1 nm tobermorite. This proves possible combination of tobermorite 1.4 nm and 1.1nm. The bands at 955 cm^{-1} (S-1) and 966 cm^{-1} (S-28) belong to Si-O lattice vibrations, while the bans at 878 cm^{-1} (S-1) and 871 cm^{-1} (S-28) belong to out of plane vibrations of the C-O. The bands at 664 cm^{-1} (S-1) and 671 cm^{-1} (S-28) probably correspond to Si-O-Si bending vibrations inside of silica chains and ν_4 SO_4^{2-} bending vibrations. These bands can be also attributed to the Si-O-Si symmetric vibration, while the bands at 494 cm^{-1} (S-1) and 509 cm^{-1} (S-28) belong to the out-of-plane bending vibration of SiO_4. Finally, the bands at 406 cm^{-1} (S-1) and 414 cm^{-1} (S-28) belong to the deformations of the SiO_4 tetrahedra.

3.3. Hydration process of calcium silicate pastes

The most important process for setting and mechanical properties of calcium silicate phases is the rate of their hydration. As it is well-known from the hydration theory of cement pastes, the hydration of β-C_2S and C_3S phases is the most important process for curing those phases during their ageing inside of water solution. It seems, following various reference sources [10, 12-15], that the reaction between C_3S and water is the main factor in the setting and hardening of cement mixtures. During this reaction, calcium silicate grains inside of mixture are wetted, causing a rapid release of Ca^{2+} and OH^- ions from each grain surface. In this process, transformation of C_3S in amorphous calcium silicate hydrate (C-S-H), well-known as tobermorite gel, and calcium hydroxide ($Ca(OH)_2$) occurs through reaction with water given by Eq(1):

$$2C_3S + 7H_2O \rightarrow C\text{-}S\text{-}H + 3CH. \quad (1)$$

Similarly, reaction between β-C_2S and water gives C-S-H and $Ca(OH)_2$, as it is shown in Eq(2):

$$2C_2S + 5H_2O \rightarrow C\text{-}S\text{-}H + CH \quad (2)$$

The obtained amorphous C-S-H can have variable composition (C: S varies with the concentration of released OH^- ions). The number of water molecules bound to product of hydrate gel is also variable. It is expected that the most of $Ca(OH)_2$ might be crystalline. Smaller XRD peaks for characteristic planes of portlandite, present in all samples, indicated that $Ca(OH)_2$ might be prevailing amorphous phase, found on the surface of tobermorite phase (gel). Following the hydration theory of calcium silicates, it can be assumed that overall hydration process proceeds with several steps, which can be roughly summarized in reaction, given by Eq(3) [10, 12-15]:

$$Ca_3SiO_5 + (3+y-x)H_2O \rightarrow (CaO)_x\,(SiO_2)\cdot(H_2O)_y + (3-x)Ca(OH)_2, \quad (3)$$

where x determines Ca to Si ratio of Ca-S-H and y is the sum of OH^- ions and bound water molecules that are incorporated into C-S-H structure. Both x and y vary throughout the reaction causing variation in the C-S-H composition. The composition of C-S-H gel is believed to be responsible for the strength of cured pastes. Previous reaction of formation of C-S-H gel is consisted from several steps, following Eqs. (4) and (5):

$$Ca_3SiO_5 + 3H_2O \rightarrow 3Ca^{2+} + 4OH^- + H_2SiO_4^{2-} \quad (4)$$

and

$$H_2SiO_4^{2-} + xCa^{2+} + (2x-2)OH^- + (y-x)H_2O \rightarrow (CaO)_x(SiO_2)\cdot(H_2O)_y \quad (5)$$

The ratio Ca/Si in C-S-H varies with hydration time and temperature (mostly is between 1 and 2). In agreement with Eq(5), the precipitation of $Ca(OH)_2$ results when critical concentration of Ca^{2+} ions has been reached, following Eq(6) [10, 12-15]:

$$Ca^{2+} + 2OH^- \rightarrow [Ca(OH)_2]_{(s)}. \quad (6)$$

The C-S-H produced in both reactions was the high-lime end-member of a series of hydrates designated by Taylor as calcium silicate hydrate (I) or CSH(1). Bernal tentatively assigned the structural formula $Ca_2[SiO_2(OH)_2]_2$ $[Ca(OH)_2]$ to this compound. Also, it has been long known that the hydration of C_3S in paste form is much faster than that of β-C_2S. Besides, the obtained amount of $Ca(OH)_2$ phase during the hydration is frequently significantly less then it is theoretically expected. This discrepancy can be assigned to the adsorption of $Ca(OH)_2$ on the surface of the C-S-H, to high degree of present amorphous or very poorly crystallized phase, or its partial participation inside of calcium silicate hydrate phase [10, 12-19].

Considering the XRD data and taking into account the differences between the surface areas under corresponding characteristics peaks, it is possible to show more exactly the improvement of calcium silicate phase hydration. After one day hydration, the reaction can be written in the form:

$$C_3S + 3H_2O = 0.67CaO0.17Ca(OH)_2SiO_2\cdot 0.67H_2O + 2.16Ca(OH)_2 \quad (7)$$

and

$$C_2S + 2H_2O = 0.67CaO0.17Ca(OH)_2SiO_2\cdot 0.67H_2O + 1.16\ Ca(OH)_2 \quad (8)$$

Taking into account that the ratio between C_3S and C_2S=2:1, it follows:

$$0.66C_3S + 0.33C_2S + 2.64H_2O = 0.67CaO0.17Ca(OH)_2SiO_2\cdot 0.67H_2O + 1.81Ca(OH)_2 \quad (9)$$

The degree of transformation in tobermorite, obtained by comparison of surface under the peak of characteristic plane (-2-21) between S-1 and S-28, was found to be 0.85. Accordingly, the reaction after one day can be expressed by:

$$0.66C_3S + 0.33C_2S + 2.64H_2O = 0.85[0.67CaO0.17Ca(OH)_2SiO_2\cdot 0.67H_2O] + 1.91Ca(OH)_2 + 0.15SiO_2 \quad (10)$$

After the hydration for 3 or 7 days, degree of transformation in tobermorite was 0.95, and corresponding reaction can be written in the form:

$$0.66C_3S + 0.33C_2S + 2.67H_2O = 0.95[0.67CaO0.17Ca(OH)_2SiO_2\cdot 0.67H_2O] + 1.84\ Ca(OH)_2 + 0.05SiO_2 \quad (11)$$

Finally, after 28 days of hydration, the reaction can be written as follows:

$$0.66C_3S + 0.33C_2S + 2.64H_2O = 0.67CaO0.17Ca(OH)_2SiO_2\cdot 0.67H_2O + 1.81Ca(OH)_2 \quad (12)$$

These data clearly show that, beside tobermorite, the main phase during the hydration was $Ca(OH)_2$, which is adsorbed on the surface of tobermorite, as mostly amorphous layer. The presence of crystalline portlandite phase is almost negligible, while the small amounts of unreacted amorphous silicate phase is also probably present.

4. Conclusions

The advantages of synthesis of active silicate phases by combined sol gel and high-temperature self-propagating wave method, for the first time applied in this paper, are clearly shown. The obtained nanostructured silicate phases are very active. They show significant increase of setting properties of active silicate phase, as the most important phase in any endodontic mixture.

Process of hydration of calcium silicate phases is carefully analyzed by XRD and FTIR, from the aspect of structural changes inside of mixture during its wetting for 1, 3, 7 and 28 days. After 3 days, β-C_2S and C_3S phases were mostly transformed into tobermorite, while after 7 day they were completely transformed.

The morphological characteristics of the given phase are investigated by SEM, while the uniformity of chemical composition is analyzed by EDS. It was shown that calcium silicate mixture is consisted preferentially of agglomerates with sizes of a several micrometers, built up from particles of spherical or ellipsoidal shape, more or less elongated along one direction, with dimensions between 117 and 477 nm.

Acknowledgement

This study was financially supported by the Ministry of Education and Science of the Republic of Serbia (Project No. 172026).

5. References

1. M. Torabinejad, T. F. Watson, T. R. Pitt Ford, Sealing ability of a Mineral Trioxide Aggregate when used as a root end, filling material. Journal of Endodontics 19 (1993) 591–595.
2. H. W. Roberts, J. M. Toth, D. W. Berzins, D. G. Charlton, Mineral trioxide aggregate material use in endodontic treatment: A review of the literature, Dental materials 24 (2008) 149–164.
3. J. O. Andreasen, E. C. Munksgaard, L. K. Bakland, Comparison of fracture resistance in root canals of immature sheep teeth after filling with calcium hydroxide or MTA, Dent Trauma 22 (2006) 154–56.
4. G. Bergenholtz, C. F. Cox, W. J. Loesche, S.A. Syed, Bacterial leakage around dental restoration: Its effect on the dental pulp, J.Oral.Pathol. 11 (1982) 439-450.
5. A. Khayat, A. Abbasi, N. Tanideh, A comparative study of dentin bridge formation following pulpotomy using calcium hydroxide and mineral trioxide aggregate in young dogs, Iranian J. Veterinary Res, 5 (2004) 1383-1390.
6. M. Torabinejad, N. Chivian, Clinical applications of mineral trioxide aggregate, J. Endod. 25 (1999) 197-205
7. Y. L. Lee, B. S. Lee, F. H. Lin, A. Y. Lin, W. H. Lan, C. P. Lin, Effects of physiological environments on the hydration behavior of mineral trioxide aggregate. Biomaterials 25 (2004) 787–793.
8. N. K. Sarkar, R. Caidedo, P. Tirwik, R. Moiseyeva, I. Kawashima,. Physicochemical basis of the biologic properties of mineral trioxide aggregate, J. Endod. 31 (2005) 97–100
9. R. C. Lee R. L. Feinbaum, V. Ambros, The C. elegans heterochronic gene lin-4 encodes small RNAs with antisense complementarity to lin-14, Cell 75 (1993) 843-854.
10. Jokanović, V., Dramićanin, M.D., Andrić, Z., Jokanović, B., Nedić, Z., Spasic, A.M. Luminescence properties of SiO_2:Eu^{3+} nanopowders: Multi-step nano-designing, Journal of Alloys and Compounds 453 (1-2) (2008) 253-260.
11. U. Al-Amani, S. Sreekantan, M.N. Ahmad Fauzi, A.R. Khairunisak, K. Warapong, Soft Combustion Technique: Solution Combustion Synthesis and Low-Temperature Combustion Synthesis; to Prepare Bi4Ti3O12 Powders and Bulk Ceramics, Science of Sintering 44 (2012) 211-221.
12. J. A. Nuth, Metamorphism of Cosmic Dust: Diagnostic Infrared Signatures, Astrochemistry of Cosmic Phenomena: Proceedings of the 150th Symposium of the International Astronomical Union, NASA Goddad Place Flight Center, PD Ed. Singh, 39-40, Greenbelt, MD 20771.
13. X. Cong, R. J. Kirkpatrick, ^{29}Si MAS study of the structure of calcium silicate hydrate, Adv. Cem. Based Mater. 3 (1996) 144–156.

14. W. Chen, W. Xu, Y. Li, Microstructural investigation of carbonation od calcium silicate hydrate in hydrated cement paste, Advanced Materials Research 261-263 (2011) 601-605.
15. S. N. Ghosh, S. K. Hando, Infrared and Raman spectral studies in cement and concrete (review), Cement and Concrete Research, 10 (1980) 771–782.
16. F. Ridi, E. Fratini, S. Milani, P. Baglioni, Near-Infrared Spectroscopy Investigation of the Water Confined in Tricalcium Silicate Pastes, J. Phys. Chem. 110 (2006) 16326–16331.
17. P. Yu, R. J. Kirkpatrick, B. Poe, P. F. McMillan, X. Cong, Structure of Calcium Silicate Hydrate (C-S-H): Near-, Mid-, and Far-Infrared Spectroscopy, Journal of the American Ceramic Society, 82 (1999) 742–748.
18. E. Bonaccorsi, S. Merlino, H. F. W.Taylor, The crystal structure of jennite, $Ca_9Si_6O_{18}(OH)_6{\cdot}8H_2O$, Cement and Concrete Research 34 (2004) 1481–1488.
19. S. V. Churakov, Structure of the interlayer in normal 11 Å tobermorite from an ab initio study, European Journal of Mineralogy 21 (2009) 261-271.

Садржај: *У овом раду описана је синтеза активних силикатних фаза комбиновањем сол-гел методе и високо-температурне методе самораспростирућих таласа сагоревања, Ове фазе показују значајно смањење времена везивања и добра механичка својства, која су јако важна за њихову потенцијалну примену у ендооднтској пракси.*

Процес хидратације калцијум-силикатних фаза пажљиво је анализиран са аспекта фазних промена за време њиховог потапања у воду на 1, 3, 7 или 28 дана. Метода дифракције Х-зрака и инфрацрвена спектроскопија коришћене су за фазну анализу узорака, док су морфолошка својства и хемијски састав датих фаза испитивани помоћу скенирајуће електронске микроскопије и енергетски дисперзивне спектроскопије.

Кључне речи*: калцијум-силикати, ендодонција, време везивања, притисна чврстоћа, XRD*